Hindawi
Wireless Communications and Mobile Computing
Volume 2018, Article ID 3981048, 11 pages
https://doi.org/10.1155/2018/3981048

Research Article

Low Complexity Pilot Allocation Scheme for a Large OFDM Block with Null Subcarriers

Janghyun Kim,[1] Unil Yun,[2] Duckdong Hwang,[3] and Eunchul Yoon[1]

[1] *Department of Electrical and Electronics Engineering, Konkuk University, Seoul, Republic of Korea*
[2] *Department of Computer Engineering, Sejong University, Seoul, Republic of Korea*
[3] *Department of Electronics, Information and Communication Engineering, Sejong University, Seoul, Republic of Korea*

Correspondence should be addressed to Eunchul Yoon; ecyoon@konkuk.ac.kr

Received 25 December 2017; Revised 25 February 2018; Accepted 4 March 2018; Published 10 April 2018

Academic Editor: Donatella Darsena

A low complexity pilot allocation scheme is proposed for a large OFDM block with null subcarriers. The proposed scheme allocates pilots to the edge part of the active subcarrier region according to the 2nd order polynomial and to the middle part of the active subcarrier region according to the 1st order polynomial or the comb-type pilot pattern. To find a parameter of the 2nd order polynomial, the proposed scheme applies exhaustive search of a single parameter by using an integer unit resolution. It is shown by simulation that the proposed scheme is a close-to-optimal pilot allocation scheme yielding better symbol error rate (SER) performance than the traditional 3rd and 5th order polynomial-based schemes although the proposed scheme has lower computation and implementation complexity.

1. Introduction

Orthogonal frequency division multiplexing (OFDM) is an attractive transmission technique for broadband communications. Since OFDM is appropriate for high spectral efficiency and scalable to low complexity receivers, it is well suited for the 5G cellular network [1]. It has been well known that the comb-type pilot pattern with equal pilot spacing leads to minimum mean square error (MSE) of the least-square- (LS-) based channel estimation [2]. The comb-type pilot pattern was applied to OFDM systems with multiple antennas [3]. However, the OFDM block usually includes null subcarriers for the purpose of guard band [4, 5]. Given null subcarriers, the channel estimation with the comb-type pilot pattern incurs severe channel estimation error at the edge part of the active subcarrier region [6, 7]. Recently, the international telecommunications union announced the minimum requirements related to technical performance for IMT-2020 radio interfaces, which indicated that a very large bandwidth up to 1 GHz will be used for future mobile communications [8]. Given a large OFDM block with null subcarriers, allocating pilots to the OFDM block becomes a more crucial issue. The minimum mean square error- (MMSE-) based channel estimation may suppress the channel estimation error at the edge part of the active subcarrier region effectively. However, the static pilot locations cannot be optimized by minimizing the MSE of the MMSE-based channel estimation because the MSE of the MMSE-based channel estimation is dependent on time-varying channel and noise statistics [4, 9]. Therefore, static pilot locations are usually optimized with respect to the LS-based channel estimation. In order to minimize the MSE of the LS-based channel estimation, the 3rd order polynomial-based pilot allocation was suggested in [10], which applied exhaustive search of a single parameter by using a fractional unit resolution. While the 3rd order polynomial-based pilot allocation showed good channel estimation performance for an OFDM block size 512, it incurred considerable performance degradation for an OFDM block size 1024. In [11], the optimal pilot powers were numerically computed by minimizing l_∞ norm of the channel estimate error, and the optimal pilot locations were iteratively found by symmetrically removing a certain number of insignificant pilot candidates. However, its algorithm was not optimal because it was heuristically chosen and it caused high complexity due to iteration. In [12], the 5th order polynomial-based pilot allocation was suggested. Differently from the 3rd order polynomial-based pilot allocation, the 5th order polynomial-based pilot allocation performed well with both the OFDM block sizes, 512 and 1024. In [13], the 5th order polynomial-based pilot allocation was also applied to MIMO-OFDM systems. However, the 5th order polynomial-based pilot allocation requires more complicated implementation than the 3rd order polynomial-based pilot allocation because the 5th order polynomial-based pilot allocation applies exhaustive search of two parameters by using two fractional unit resolutions. Moreover, according to our simulation results, the performance of the 5th order polynomial-based pilot allocation tends to be degraded as the OFDM block size increases further than 1024. It is because a single polynomial function cannot determine the optimal pilot locations precisely for a large OFDM block.

In this paper, a low complexity pilot allocation scheme is proposed for a large OFDM block with null subcarriers. The proposed scheme allocates pilots to the edge part of the active subcarrier region according to the 2nd order polynomial and to the middle part of the active subcarrier region according to the 1st order polynomial or the comb-type pilot pattern. To find a parameter of the 2nd order polynomial, the proposed scheme applies exhaustive search of a single parameter by using an integer unit resolution. It is shown by simulation that the proposed scheme is a close-to-optimal pilot allocation scheme yielding better symbol error rate (SER) performance than the traditional 3rd and 5th order polynomial-based schemes for all the OFDM block sizes although it has lower computation and implementation complexity.

2. System Model

An OFDM system with an OFDM block size N is considered, where the set of the subcarrier indices is given by $\{0, 1, \ldots, N-1\}$. Let N_n and N_a define the number of null subcarriers and that of active subcarriers in the OFDM block, respectively. The N_a active subcarriers are divided into N_p pilot subcarriers and N_d data subcarriers. Let $\mathcal{S}_\mathrm{p} = \{p_0, p_1, \ldots, p_{N_\mathrm{p}-1}\}$ and $\mathcal{S}_\mathrm{d} = \{d_0, d_1, \ldots, d_{N_\mathrm{d}-1}\}$ define the index set of N_p pilot subcarriers and that of N_d data subcarriers, respectively. It is assumed that the channel impulse response is composed of L multipaths as

$$\mathbf{h} = \left[h_0, h_1, \ldots, h_{L-2}, h_{L-1}\right]^T, \tag{1}$$

where $(\cdot)^T$ denotes the transpose operator. The channel frequency response coefficient vectors for the pilot and data subcarriers can be written as

$$\mathbf{H}_\mathrm{p} = \mathbf{D}_\mathrm{p}\mathbf{h}, \tag{2}$$

$$\mathbf{H}_\mathrm{d} = \mathbf{D}_\mathrm{d}\mathbf{h}, \tag{3}$$

where $\mathbf{D}_\mathrm{p}$ and $\mathbf{D}_\mathrm{d}$ denote two Vandermonde matrices given by $[\mathbf{D}_\mathrm{p}]_{k,l} = e^{-j(2\pi/N)p_k l}$ for $0 \le k \le N_\mathrm{p}-1$, $0 \le l \le L-1$, and $[\mathbf{D}_\mathrm{d}]_{n,l} = \mathrm{e}^{-j(2\pi/N)d_n l}$ for $0 \le n \le N_\mathrm{d}-1$, $0 \le l \le L-1$, while $[\mathbf{D}]_{k,l}$ denotes the element of a matrix $\mathbf{D}$ in the kth row and the lth column. To apply the LS-based channel estimation, the number of the pilots N_p should be greater than or equal to the channel length L. For the purpose of achieving maximum frequency efficiency, it is assumed that $N_\mathrm{p} = L$. Let $\mathbf{X}_\mathrm{d}$ and $\mathbf{X}_\mathrm{p}$ define the transmitted data symbol vector and the pilot symbol vector, respectively. In addition, let $\mathrm{diag}\{\mathbf{X}\}$ define a diagonal matrix with its diagonal components given by the components of $\mathbf{X}$ when $\mathbf{X}$ is a column vector and let $\mathrm{diag}\{\mathbf{X}\}$ define a column vector with its components given by the diagonal components of $\mathbf{X}$ when $\mathbf{X}$ is a diagonal matrix. Then, the received signal vector over the pilot subcarriers can be written as

$$\mathbf{Y}_\mathrm{p} = \mathrm{diag}\left\{\mathbf{X}_\mathrm{p}\right\}\mathbf{H}_\mathrm{p} + \mathbf{W}_\mathrm{p}, \tag{4}$$

where $\mathbf{W}_\mathrm{p}$ denotes a zero mean circularly symmetric complex Gaussian noise vector with component wise variance σ^2. Under the assumption that the data and pilot symbols have unitary average power, SNR is defined by $1/\sigma^2$. The channel frequency response coefficient vector over the pilot subcarriers is estimated by $\widehat{\mathbf{H}}_\mathrm{p} = \mathrm{diag}\{\mathbf{X}_\mathrm{p}\}^{-1}\mathbf{Y}_\mathrm{p}$ to give

$$\widehat{\mathbf{H}}_\mathrm{p} = \mathbf{H}_\mathrm{p} + \mathrm{diag}\left\{\mathbf{X}_\mathrm{p}\right\}^{-1}\mathbf{W}_\mathrm{p}. \tag{5}$$

The channel frequency response coefficient vector for the data subcarriers is estimated by using the LS method [14] as

$$\widehat{\mathbf{H}}_\mathrm{d} = \mathbf{D}_\mathrm{d}\left(\mathbf{D}_\mathrm{p}^H\mathbf{D}_\mathrm{p}\right)^{-1}\mathbf{D}_\mathrm{p}^H\widehat{\mathbf{H}}_\mathrm{p}, \tag{6}$$

where $(\cdot)^H$ denotes the transpose complex conjugate operator. Note that as N_p increases, the matrix $\mathbf{D}_\mathrm{p}^H\mathbf{D}_\mathrm{p}$ as shown in (6) becomes ill-conditioned to be a nearly singular matrix. In such a case, the inverse of the matrix $\mathbf{D}_\mathrm{p}^H\mathbf{D}_\mathrm{p}$ can be computed by using the Moore-Penrose inverse [15]. The Moore-Penrose inverse computes a best fit solution to a system of linear equations that lacks a unique solution. A simple way of describing the Moore-Penrose inverse is the singular value decomposition. Let $\mathbf{A} = \mathbf{U}\Sigma\mathbf{V}^H$ define the singular value decomposition of a square matrix $\mathbf{A}$, where $\mathbf{U}$ and $\mathbf{V}$ are two unitary matrices and Σ is a diagonal matrix. The Moore-Penrose inverse of $\mathbf{A}$ is given by $\mathbf{U}\Sigma^\dagger\mathbf{V}^H$, where the diagonal matrix $\Sigma^\dagger$ is obtained by changing the diagonal components of Σ smaller than some small tolerance to zeros and taking the reciprocal numbers of the other diagonal components. From (2) and (5), the channel impulse response can be estimated by

$$\hat{\mathbf{h}} = \mathbf{h} + \mathbf{D}_\mathrm{p}^{-1}\mathrm{diag}\left\{\mathbf{X}_\mathrm{p}\right\}^{-1}\mathbf{W}_\mathrm{p}. \tag{7}$$

Then, the channel frequency response coefficient vector for the data subcarriers is estimated by

$$\widehat{\mathbf{H}}_\mathrm{d} = \mathbf{H}_\mathrm{d} + \mathbf{D}_\mathrm{d}\mathbf{D}_\mathrm{p}^{-1}\mathrm{diag}\left\{\mathbf{X}_\mathrm{p}\right\}^{-1}\mathbf{W}_\mathrm{p}. \tag{8}$$

If the components of $\mathbf{X}_p$ have uniform pilot powers, the MSE vector of the LS-based channel estimation for the data subcarriers can be written as

$$\mathbf{e} = \sigma^2\,\mathrm{diag}\left\{\mathbf{D}_\mathrm{d}\left(\mathbf{D}_\mathrm{p}^H\mathbf{D}_\mathrm{p}\right)^{-1}\mathbf{D}_\mathrm{d}^{\;H}\right\}. \tag{9}$$

The averaged MSE over all the N_{d} data subcarriers can be written as

$$\xi = \frac{\sigma^2}{N_{\mathrm{d}}} \operatorname{tr}\left\{\mathbf{D}_{\mathrm{d}}\left(\mathbf{D}_{\mathrm{p}}^H\mathbf{D}_{\mathrm{p}}\right)^{-1}\mathbf{D}_{\mathrm{d}}{}^H\right\}, \tag{10}$$

where $\operatorname{tr}\{\cdot\}$ denotes the trace operator. Since optimizing the pilot locations through ξ minimization is not affected by the value of σ^2, the scaled MSE given by

$$\frac{\xi}{\sigma^2} = \frac{1}{N_{\mathrm{p}}} \operatorname{tr}\left\{\left(\frac{1}{N_{\mathrm{p}}}\mathbf{D}_{\mathrm{p}}^H\mathbf{D}_{\mathrm{p}}\right)^{-1}\left(\frac{1}{N_{\mathrm{d}}}\mathbf{D}_{\mathrm{d}}{}^H\mathbf{D}_{\mathrm{d}}\right)\right\} \tag{11}$$

can be used for finding the optimal pilot locations. The quantities $(1/N_{\mathrm{d}})\mathbf{D}_{\mathrm{d}}^H\mathbf{D}_{\mathrm{d}}$ and $(1/N_{\mathrm{p}})\mathbf{D}_{\mathrm{p}}^H\mathbf{D}_{\mathrm{p}}$ in (11) are $N_{\mathrm{p}} \times N_{\mathrm{p}}$ dimensional square matrices, whose diagonal components are given by 1's. By applying the singular value decomposition, those quantities can be written as

$$\begin{aligned}\frac{1}{N_{\mathrm{p}}}\mathbf{D}_{\mathrm{p}}^H\mathbf{D}_{\mathrm{p}} &= \mathbf{U}_{\mathrm{p}}\Lambda_{\mathrm{p}}\mathbf{U}_{\mathrm{p}}^H, \\ \frac{1}{N_{\mathrm{d}}}\mathbf{D}_{\mathrm{d}}^H\mathbf{D}_{\mathrm{d}} &= \mathbf{U}_{\mathrm{d}}\Lambda_{\mathrm{d}}\mathbf{U}_{\mathrm{d}}^H,\end{aligned} \tag{12}$$

where $\mathbf{U}_{\mathrm{p}}$ and $\mathbf{U}_{\mathrm{d}}$ denote unitary matrices and Λ_{p} and Λ_{d} denote diagonal matrices. By defining $\mathbf{V} = \mathbf{U}_{\mathrm{d}}^H\mathbf{U}_{\mathrm{p}}$ with $\mathbf{v}_k$ being its kth column and $\omega_k = \mathbf{v}_k^H\Lambda_{\mathrm{d}}\mathbf{v}_k$ for $k = 0, 1, \ldots, N_{\mathrm{p}} - 1$, the scaled MSE reduces to

$$\frac{\xi}{\sigma^2} = \frac{1}{N_{\mathrm{p}}}\sum_{k=0}^{N_{\mathrm{p}}-1}\frac{\omega_k}{\lambda_k}, \tag{13}$$

where λ_k is the kth diagonal component of Λ_p. Since ω_k is formed by a weighted sum of the eigenvalues of $(1/N_{\mathrm{d}})\mathbf{D}_{\mathrm{d}}^H\mathbf{D}_{\mathrm{d}}$, it is more critical to prevent a very small eigenvalue of $(1/N_{\mathrm{p}})\mathbf{D}_{\mathrm{p}}^H\mathbf{D}_{\mathrm{p}}$ than that of $(1/N_{\mathrm{d}})\mathbf{D}_{\mathrm{d}}^H\mathbf{D}_{\mathrm{d}}$ in order to reduce the scaled MSE. Due to the existence of the null subcarrier region, the comb-type pilot pattern is prone to induce a small minimum eigenvalue of $(1/N_{\mathrm{p}})\mathbf{D}_{\mathrm{p}}^H\mathbf{D}_{\mathrm{p}}$ and incur a large MSE result. Therefore, if the OFDM block includes the null subcarrier region, pilots should be allocated to the active subcarrier region in efforts to maximize the minimum eigenvalue of $(1/N_{\mathrm{p}})\mathbf{D}_{\mathrm{p}}^H\mathbf{D}_{\mathrm{p}}$.

3. Proposed Pilot Allocation Scheme

Figure 1 shows the structure of the OFDM block that consists of the null subcarrier region and the active subcarrier region. The active subcarrier region is divided into a middle part and two edge parts. The edge part represents a boundary part of the active subcarrier region, which incurs comparatively large MSEs when pilots are allocated to the active subcarrier region according to the comb-type pilot pattern. To effectively suppress the MSEs at both the edge and middle parts, the numbers of the pilots allocated to the edge and middle parts should be well balanced. In particular, since the detrimental impact of the null subcarrier region on the pilot-based channel estimation dissipates as the subcarrier distance from the null subcarrier region increases, a gradually changing pilot density should be applied to the edge part and a uniform pilot density should be applied to the middle part for better performance. Therefore, we propose to apply two separate polynomials to the edge and middle parts. Let N_{e} and N_{ep} define the number of the one-sided edge part subcarriers and that of pilots allocated to the one-sided edge part, respectively. In the proposed scheme, N_{ep} pilots are allocated to the edge part according to the 2nd order polynomial and $N_{\mathrm{p}} - 2N_{\mathrm{ep}}$ pilots are allocated to the middle part according to the 1st order polynomial. Therefore, the subcarrier indices of the first $N_{\mathrm{p}}/2$ pilots are chosen by

$$n_k = \begin{cases}\left\lfloor a_1k^2 + a_2k + a_3\right\rfloor & \text{for } k = 0, 1, \ldots, N_{\mathrm{ep}}, \\ \lfloor mk + b\rfloor & \text{for } k = N_{\mathrm{ep}}, N_{\mathrm{ep}} + 1, \ldots, \dfrac{N_{\mathrm{p}}}{2} - 1,\end{cases} \tag{14}$$

where k denotes the pilot index, n_k denotes the subcarrier index of the kth pilot, and $\lfloor\cdot\rfloor$ denotes the floor operator. From Figure 1, it is easy to infer the following five conditions for the 1st and 2nd order polynomials:

$$mk + b\big|_{k=N_{\mathrm{ep}}-1} = \frac{N_{\mathrm{n}}}{2} + N_{\mathrm{e}} - 1, \tag{15}$$

$$mk + b\big|_{k=N_{\mathrm{p}}-N_{\mathrm{ep}}} = N - \frac{N_{\mathrm{n}}}{2} - N_{\mathrm{e}}, \tag{16}$$

$$a_1k^2 + a_2k + a_3\big|_{k=0} = \frac{N_{\mathrm{n}}}{2}, \tag{17}$$

$$a_1k^2 + a_2k + a_3\big|_{k=N_{\mathrm{ep}}-1} = \frac{N_{\mathrm{n}}}{2} + N_{\mathrm{e}} - 1, \tag{18}$$

$$a_1k^2 + a_2k + a_3\big|_{k=N_{\mathrm{ep}}} = mN_{\mathrm{ep}} + b. \tag{19}$$

From (15) and (16), the coefficients of the 1st order polynomial, m and b, can be found as

$$m = \frac{N_{\mathrm{a}} - 2N_{\mathrm{e}} + 1}{N_{\mathrm{p}} - 2N_{\mathrm{ep}} + 1}, \tag{20}$$

$$b = \frac{N-1}{2} - \frac{\left(N_{\mathrm{p}} - 1\right)\left(N_{\mathrm{a}} - 2N_{\mathrm{e}} + 1\right)}{2\left(N_{\mathrm{p}} - 2N_{\mathrm{ep}} + 1\right)}. \tag{21}$$

From (17)–(21), the coefficients of the 2nd order polynomial, a_1, a_2, and a_3, can be found as

$$a_1 = \frac{1}{N_{\mathrm{ep}}}\left(\frac{N_{\mathrm{a}} - 2N_{\mathrm{e}} + 1}{N_{\mathrm{p}} - 2N_{\mathrm{ep}} + 1} - \frac{N_{\mathrm{e}}}{N_{\mathrm{ep}} - 1}\right), \tag{22}$$

$$\begin{aligned}a_2 = {} & \frac{\left(N_{\mathrm{e}} - 1\right)\left(2N_{\mathrm{ep}} - 1\right)}{N_{\mathrm{ep}}\left(N_{\mathrm{ep}} - 1\right)} \\ & - \frac{\left(N_{\mathrm{ep}} - 1\right)\left(N_{\mathrm{a}} - 2N_{\mathrm{e}} + 1\right)}{N_{\mathrm{ep}}\left(N_{\mathrm{p}} - 2N_{\mathrm{ep}} + 1\right)},\end{aligned} \tag{23}$$

$$a_3 = \frac{N_{\mathrm{n}}}{2}. \tag{24}$$

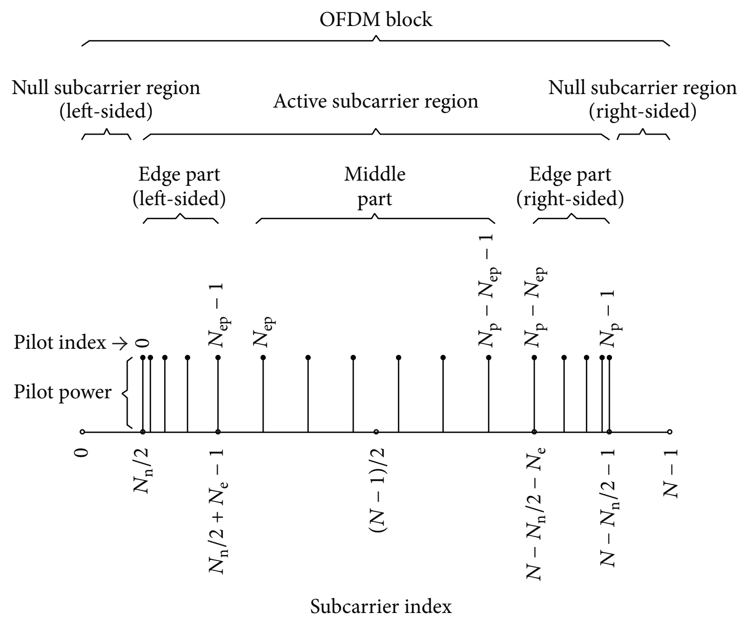

Figure 1: The structure of the OFDM block that consists of the null subcarrier region and the active subcarrier region.

The subcarrier indices for the remaining $N_p/2$ pilots with pilot indices, $k = N_p/2, N_p/2+1, \ldots, N_p-1$, can be found by using the symmetry of pilot allocation with respect to the center of the OFDM block as

$$n_k = N - 1 - n_{N_p-1-k}. \tag{25}$$

To determine the subcarrier indices of pilots based on (14) and (25), two parameters N_e and N_{ep}, which can effectively suppress the averaged MSE, should be known in advance. In the proposed scheme, N_{ep} is determined by referring to the number of the pilots that would be allocated to the one-sided edge part and the one-sided null subcarrier region if the N_p pilots were uniformly allocated to the entire OFDM block. Intuitively, this idea means that the pilots, which would belong to the null subcarrier region if the comb-type pilot pattern were applied to the entire OFDM block, are added to the edge part. This idea can be formulated as

$$\frac{N_p}{N} = \frac{N_{ep}}{N_e + N_n/2}. \tag{26}$$

The left-hand side of (26) means the pilot density when N_p pilots are uniformly allocated to the entire OFDM block, and the right-hand side of (26) means the pilot density when N_{ep} pilots are uniformly allocated to the one-sided edge part and the one-sided null subcarrier region. Given the value of N_e, the value of N_{ep} can be computed based on (26) as

$$N_{ep} = \left\lfloor \frac{N_p}{N} \times \left(N_e + \frac{N_n}{2}\right) \right\rfloor. \tag{27}$$

To compute N_{ep} based on (27), N_e should be known in advance. In the proposed scheme, the optimal value of N_e is found by applying exhaustive search through ξ/σ^2 minimization. The set of the candidate values for N_e is chosen by $\{2, 3, \ldots, N_n\}$. The 3rd order polynomial-based pilot allocation in [10] applied exhaustive search of a parameter by using a fractional unit resolution, and the 5th order polynomial-based pilot allocation in [12] applied exhaustive search of two parameters by using two fractional unit resolutions. The proposed scheme has lower optimization complexity than both the 3rd and 5th order polynomial-based pilot allocation schemes because the proposed scheme applies exhaustive search of a single parameter (i.e., N_e) by using an integer unit resolution.

4. Numerical Results

In this section, the proposed pilot allocation scheme is compared to three traditional pilot allocation schemes for an OFDM block with null subcarriers. For notational convenience, the proposed scheme and the three traditional pilot allocation schemes are denoted as follows:

(i) PROPOSED represents the proposed pilot allocation scheme explained in the previous section.

(ii) POLY-5TH represents a pilot allocation scheme based on the 5th polynomial-based pilot allocation in [12].

(iii) POLY-3RD represents a pilot allocation scheme based on the 3rd polynomial-based pilot allocation in [10].

(iv) COMB represents a pilot allocation scheme based on the comb-type pilot pattern with equal pilot spacing.

In addition, for reference purposes only, the proposed pilot allocation scheme is compared to the following scheme:

(v) NO-NULLSUBC represents a comb-type pilot allocation scheme in the case of $L = N_p$ assuming that the OFDM block includes no null subcarrier. If the pilot number is $\widetilde{N}_p$, the pilot spacing and the data subcarrier number are given by $N/\widetilde{N}_{\mathrm{p}}$ and $\widetilde{N}_{\mathrm{d}} = N - \widetilde{N}_{\mathrm{p}}$, respectively. By adjusting $\widetilde{N}_{\mathrm{p}}$, this scheme chooses its pilot density to be equal to that of COMB. With this scheme, all the data subcarriers have the same MSE as $\sigma^2 N_{\mathrm{p}}/\widetilde{N}_{\mathrm{p}}$ (refer to the appendix). If a pilot allocation scheme locates pilots only to a limited region of the OFDM block, it is prone to induce a smaller minimum eigenvalue of $(1/N_{\mathrm{p}})\mathbf{D}_{\mathrm{p}}^H\mathbf{D}_{\mathrm{p}}$ and incur a larger MSE result than this scheme. Therefore, the MSE value of $\sigma N_{\mathrm{p}}/\widetilde{N}_{\mathrm{p}}$ can be regarded as an MSE lower-bound of COMB and other pilot allocation schemes when the OFDM block includes null subcarriers.

The components of the channel $\mathbf{h}$ are generated as circularly symmetric complex Gaussian variables with zero mean and unitary variance. The pilot power allocation method derived in [12] is applied to all the pilot allocation schemes. The transmitted symbols are selected from the QPSK constellation with unitary symbol power.

Figure 2 presents pilot allocation results from the four pilot allocation schemes when $N = 1024$, $N_{\mathrm{a}} = 942$, and $N_{\mathrm{p}} = 64$. All the pilot allocation schemes reduce the pilot power at the edge part of the active subcarrier region as the pilot subcarrier approaches the null subcarrier region. POLY-5TH, POLY-3RD, and PROPOSED allocate pilots to the edge part with a gradually changing pilot density. COMB allocates pilots to the active subcarrier region by using equal pilot spacing and nonuniform power distribution. PROPOSED allocates pilots to the middle part with equal pilot spacing and uniform pilot power distribution.

Figure 3 presents the MSEs of the data subcarrier channels from (a) PROPOSED, (b) POLY-5TH, (c) POLY-3RD, and (d) COMB when $N = 1024$, $N_{\mathrm{a}} = 942$, $N_{\mathrm{p}} = 64$, and 20 dB SNR. It can be seen that COMB yields very large MSEs at the edge part. It is because, with equally spaced pilots, the matrix $\mathbf{D}_{\mathrm{p}}^H\mathbf{D}_{\mathrm{p}}$ as shown in (10) becomes ill-conditioned to be a nearly singular matrix. However, since PROPOSED allocates pilots to the edge and middle part effectively, PROPOSED has substantially smaller MSE peaks than other pilot allocation schemes.

Figure 4 shows the impact of N on the averaged MSEs (i.e., ξ in (10)) when $N_{\mathrm{a}} = \lfloor 0.92N \rfloor$, $N_{\mathrm{p}} = N/16$, and SNR = 20 dB. It can be seen that COMB performs worse than the other pilot allocation schemes. POLY-3RD and POLY-5TH tend to have performance degradation as the value of N increases. It implies that using a single polynomial is inappropriate to find the optimal pilot locations for a large OFDM block. However, PROPOSED yields good MSE results comparable to those of NO-NULLSUBC for all the OFDM block sizes because PROPOSED uses two separate polynomials and allocates pilots to the edge and middle parts of the active subcarrier region effectively.

Figures 5 and 6 show the impact of N_{p}/N on the averaged MSEs when $N_{\mathrm{a}} = \lfloor 0.92N \rfloor$ and SNR = 20 dB in four cases of $N = 512$, $N = 1024$, $N = 2048$, and $N = 4096$. While PROPOSED yields good MSE results comparable to those of NO-NULLSUBC for all N_{p}/N values, POLY-3RD, POLY-5TH, and COMB tend to have performance degradation by increasing the N_{p}/N value. The reason for the performance degradation of POLY-3RD, POLY-5TH, and COMB is that with more of inappropriately located pilots, the matrix $\mathbf{D}_{\mathrm{p}}^H\mathbf{D}_{\mathrm{p}}$ in (11) becomes ill-conditioned to be a nearly singular matrix. It implies that using a single polynomial is inappropriate to find the optimal pilot locations for a large OFDM block.

Figures 7 and 8 show the impact of N_{a}/N on the averaged MSEs when $N_{\mathrm{p}} = N/16$ and SNR = 20 dB in four cases of $N = 512$, $N = 1024$, $N = 2048$, and $N = 4096$. While PROPOSED yields good MSE results comparable to those of NO-NULLSUBC for all the N_{a}/N values, POLY-3RD and POLY-5TH tend to have performance degradation as the N_{a}/N value increases. Since the length of the edge part decreases with a larger value of N_{a}/N, it becomes more difficult for a single polynomial to allocate pilots to the narrower edge part according to a high and gradually changing pilot density and to the wider middle part according to a uniform pilot density. However, PROPOSED can allocate pilots effectively to the edge and middle parts because PROPOSED uses two separate polynomials. For most of the N_{a}/N values, COMB performs worse than the other schemes. Given a value of N_{a}/N close to 1, the MSE results of POLY-3RD, POLY-5TH, and COMB become compatible with those of PROPOSED because a very small null subcarrier region has little impact on the pilot-based channel estimation and the optimal pilot allocation reduces to the comb-type pilot pattern.

Figure 9 presents the values of ω_k/λ_k in (13) with respect to the 16 smallest eigenvalues of $(1/N_{\mathrm{p}})\mathbf{D}_{\mathrm{p}}^H\mathbf{D}_{\mathrm{p}}$ when $N = 2048$, $N_{\mathrm{a}} = 1884$, and $N_{\mathrm{p}} = 128$. The values of ω_k/λ_k with respect to the 112 largest eigenvalues of $(1/N_{\mathrm{p}})\mathbf{D}_{\mathrm{p}}^H\mathbf{D}_{\mathrm{p}}$ were omitted in the figure because those values have insignificant difference compared to the last 16 values of ω_k/λ_k. It can be seen that PROPOSED yields smaller ω_k/λ_k values than POLY-5TH, POLY-3RD, and COMB, especially when $k \geq 125$. It is because by effectively allocating pilots to the active subcarrier region, PROPOSED makes $(1/N_{\mathrm{p}})\mathbf{D}_{\mathrm{p}}^H\mathbf{D}_{\mathrm{p}}$ have a larger minimum eigenvalue than POLY-5TH, POLY-3RD, and COMB. Since PROPOSED attains good ω_k/λ_k results which are comparable to those of NO-NULLSUBC, it is expected that using a larger number of polynomials or higher order polynomials for pilot allocation will increase optimization and implementation complexity without attaining significant performance gain over PROPOSED.

Figure 10 presents the SERs in terms of SNR in two cases of (a) $N = 512$, $N_{\mathrm{a}} = 470$, and $N_{\mathrm{p}} = 32$ and (b) $N = 1024$, $N_{\mathrm{a}} = 942$, and $N_{\mathrm{p}} = 64$. In Figure 10(a), it can be seen that with an OFDM block size 512, POLY-5TH, POLY-3RD, and PROPOSED perform almost equally while COMB performs worse than the other schemes. By comparing Figure 10(a) and 10(b), it can be seen that as the OFDM block size increases from 512 to 1024, the performance of POLY-3RD deteriorates. However, PROPOSED yields good SER results comparable to those of NO-NULLSUBC.

Figure 11 presents the SERs in terms of SNR in two cases of (a) $N = 2048$, $N_{\mathrm{a}} = 1884$, and $N_{\mathrm{p}} = 128$ and (b) $N = 4096$, $N_{\mathrm{a}} = 3768$, and $N_{\mathrm{p}} = 256$. By comparing the results in Figure 11 with those in Figure 10, it can be seen that, with a larger OFDM block, the SERs of POLY-3RD and POLY-5TH are degraded. It is because, given a larger OFDM block,

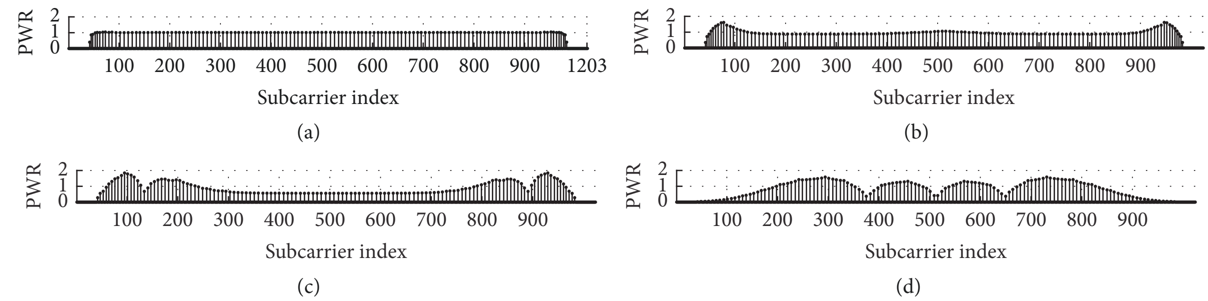

FIGURE 2: The pilot allocation results from (a) PROPOSED, (b) POLY-5TH, (c) POLY-3RD, and (d) COMB, when $N = 1024$, $N_{\mathrm{a}} = 942$, and $N_{\mathrm{p}} = 64$.

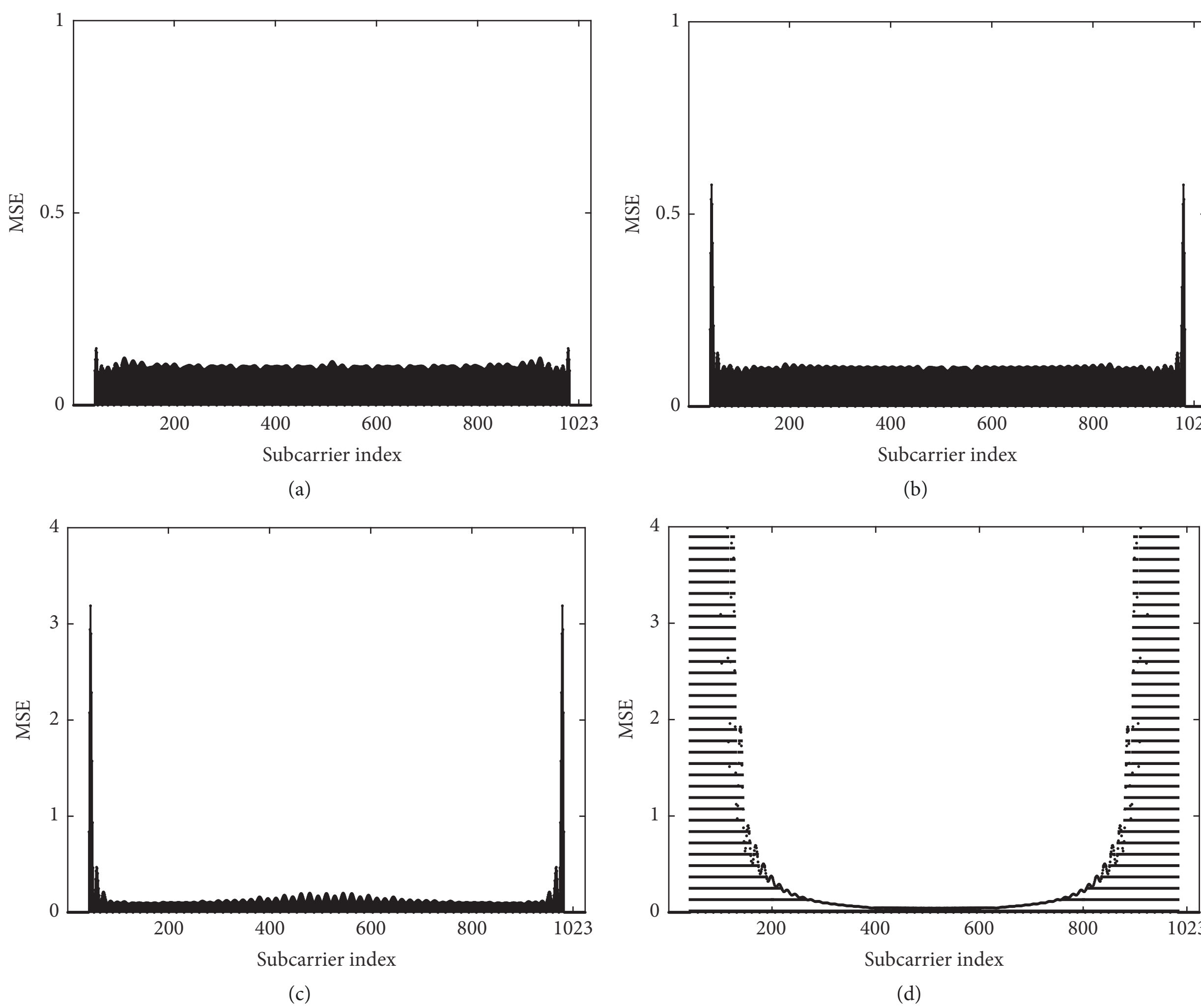

FIGURE 3: The MSEs of the data subcarrier channels from (a) PROPOSED, (b) POLY-5TH, (c) POLY-3RD, and (d) COMB when $N = 1024$, $N_{\mathrm{a}} = 942$, $N_{\mathrm{p}} = 64$, and 20 dB SNR.

it is difficult for a single polynomial to realize a changing pilot density for both the edge and middle parts effectively. However, PROPOSED yields good SER results comparable to those of NO-NULLSUBC because PROPOSED uses two polynomials.

5. Conclusion

Since the proposed scheme used two separate polynomials, it could allocate pilots to the edge and middle parts of the active subcarrier region effectively. It was shown by simulation

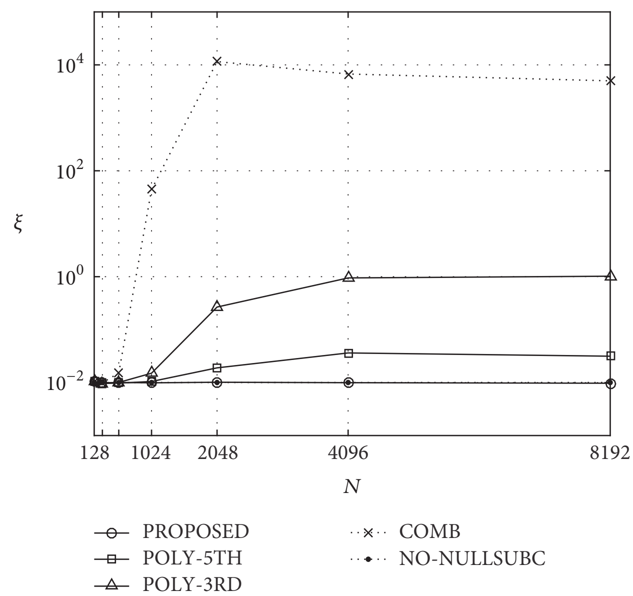

FIGURE 4: The averaged MSEs in terms of N when $N_a = \lfloor 0.92N \rfloor$, $N_p = N/16$, and SNR = 20 dB.

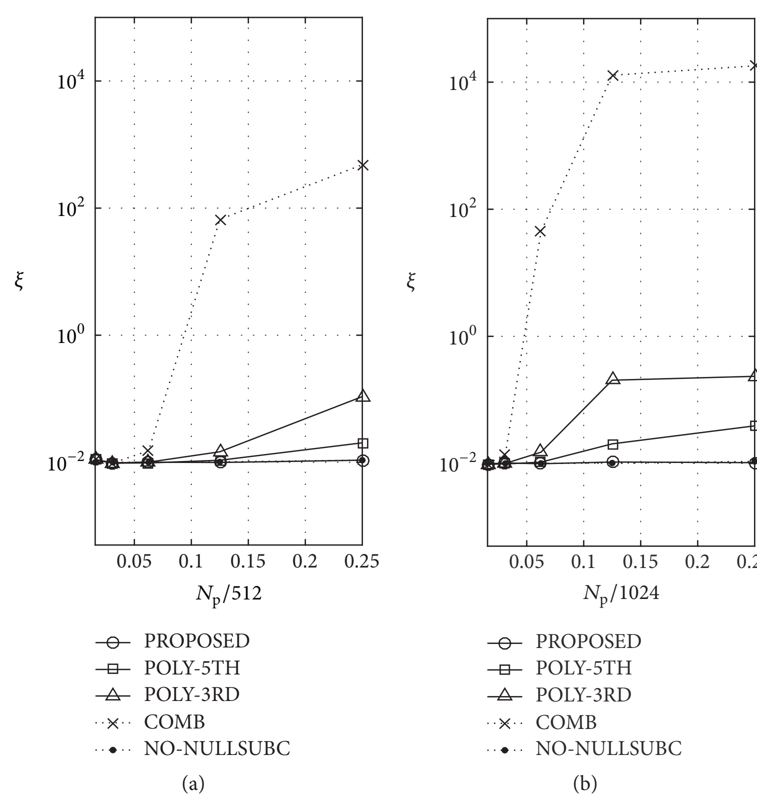

FIGURE 5: The averaged MSEs in terms of N_p/N when $N_a = \lfloor 0.92N \rfloor$ and SNR = 20 dB in the cases of (a) $N = 512$ and (b) $N = 1024$.

that the proposed scheme attained close-to-optimal channel estimation performance and outperformed the traditional 3rd and 5th order polynomial-based pilot allocation schemes for all the OFDM block sizes although the proposed scheme had lower computation and implementation complexity.

Appendix

In the following, it will be shown that if NO-NULLSUBC is applied, all the data subcarriers have the same MSE as $\sigma^2 N_p/\widetilde{N}_p$. Since NO-NULLSUBC is a pilot allocation scheme

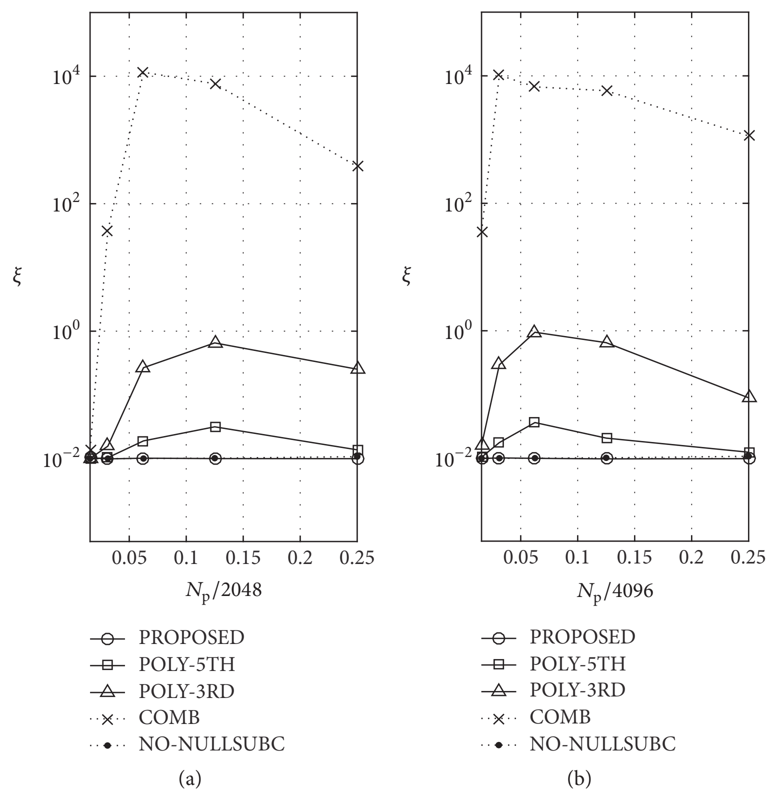

FIGURE 6: The averaged MSEs in terms of N_p/N when $N_a = \lfloor 0.92N \rfloor$ and SNR = 20 dB in the cases of (a) $N = 2048$ and (b) $N = 4096$.

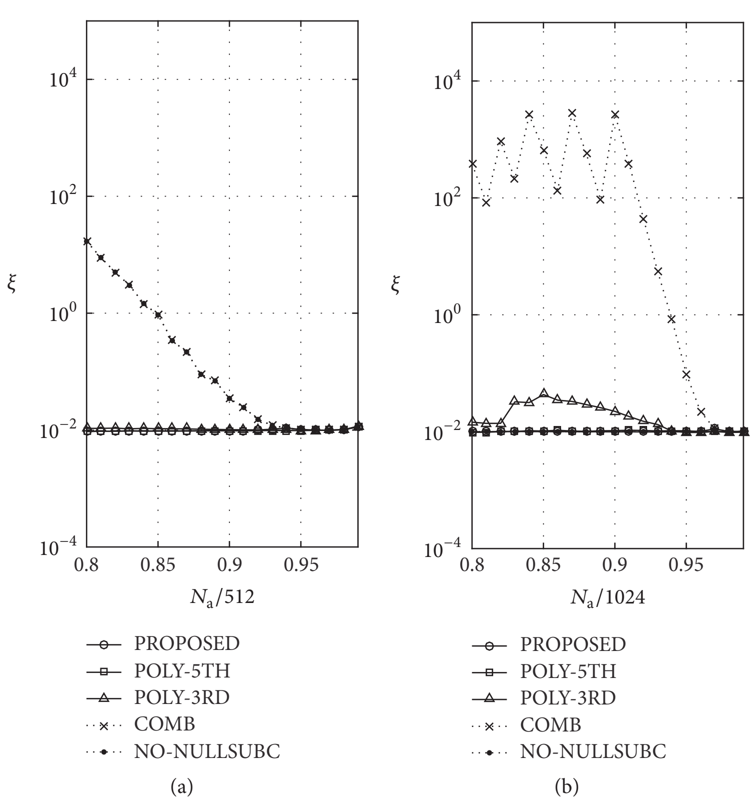

FIGURE 7: The averaged MSEs in terms of N_a/N when $N_p = N/16$ and SNR = 20 dB in the cases of (a) $N = 512$ and (b) $N = 1024$.

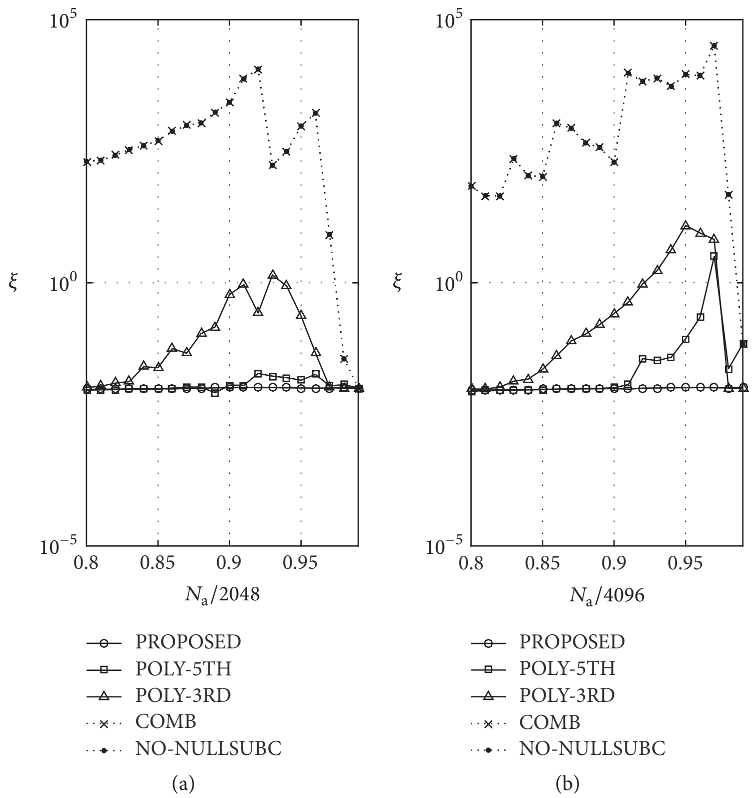

FIGURE 8: The averaged MSEs in terms of N_a/N when $N_p = N/16$ and SNR = 20 dB in the cases of (a) $N = 2048$ and (b) $N = 4096$.

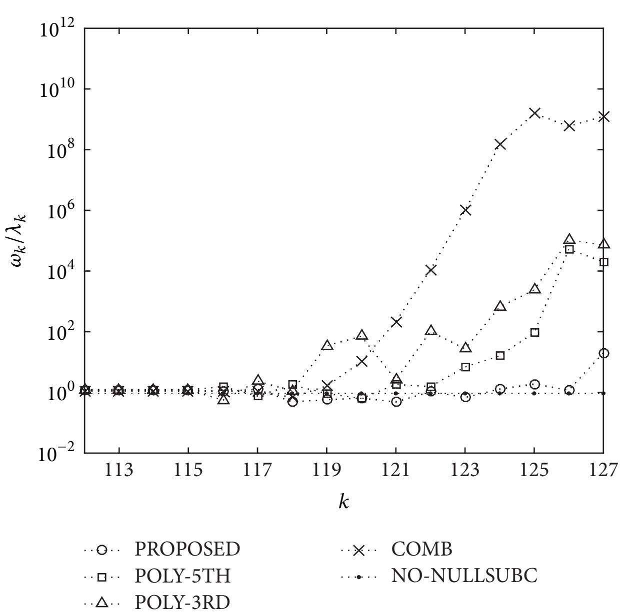

FIGURE 9: The ω_k/λ_k results as shown in (13) with respect to the 16 smallest eigenvalues of $(1/N_p)\mathbf{D}_p^H\mathbf{D}_p$ when $N = 2048$, $N_a = 1884$, and $N_p = 128$.

based on the comb-type pilot pattern for an OFDM block without null subcarriers, the pilot and data subcarrier indices can be chosen as

$$\widetilde{p}_k = \frac{kN}{\widetilde{N}_p}, \tag{A.1}$$

for $k = 0, 1, \ldots, \widetilde{N}_p - 1$ and

$$\widetilde{d}_n = n + 1 + \frac{n}{\left(N/\widetilde{N}_p - 1\right)}, \tag{A.2}$$

for $n = 0, 1, \ldots, \widetilde{N}_d - 1$. If $\widetilde{\mathbf{D}}_p$ and $\widetilde{\mathbf{D}}_d$ are two Vandermonde matrices with $[\widetilde{\mathbf{D}}_p]_{k,l} = e^{-j(2\pi/N)\widetilde{p}_k l}$ for $0 \le k \le \widetilde{N}_p - 1$, $0 \le l \le N_p - 1$, and $[\widetilde{\mathbf{D}}_d]_{n,l} = e^{-j(2\pi/N)\widetilde{d}_n l}$ for $0 \le n \le \widetilde{N}_d - 1$, $0 \le l \le N_p - 1$, the scaled MSE of NO-NULLSUBC can be written analogously to (11) as

$$\frac{\widetilde{\xi}}{\sigma^2} = \frac{1}{\widetilde{N}_p}\operatorname{tr}\left\{\left(\frac{1}{\widetilde{N}_p}\widetilde{\mathbf{D}}_p^H\widetilde{\mathbf{D}}_p\right)^{-1}\left(\frac{1}{\widetilde{N}_d}\widetilde{\mathbf{D}}_d^H\widetilde{\mathbf{D}}_d\right)\right\}. \tag{A.3}$$

From (A.1), it can be easily driven that

$$\frac{1}{\widetilde{N}_p}\left[\widetilde{\mathbf{D}}_p^H\widetilde{\mathbf{D}}_p\right]_{l_1,l_2} = \frac{1}{\widetilde{N}_p}\sum_{k=0}^{\widetilde{N}_p-1} e^{j(2\pi/\widetilde{N}_p)k(l_1-l_2)}. \tag{A.4}$$

From the orthogonality of complex exponentials, it follows that

$$\frac{1}{\widetilde{N}_p}\widetilde{\mathbf{D}}_p^H\widetilde{\mathbf{D}}_p = \mathbf{I}_{N_p}, \tag{A.5}$$

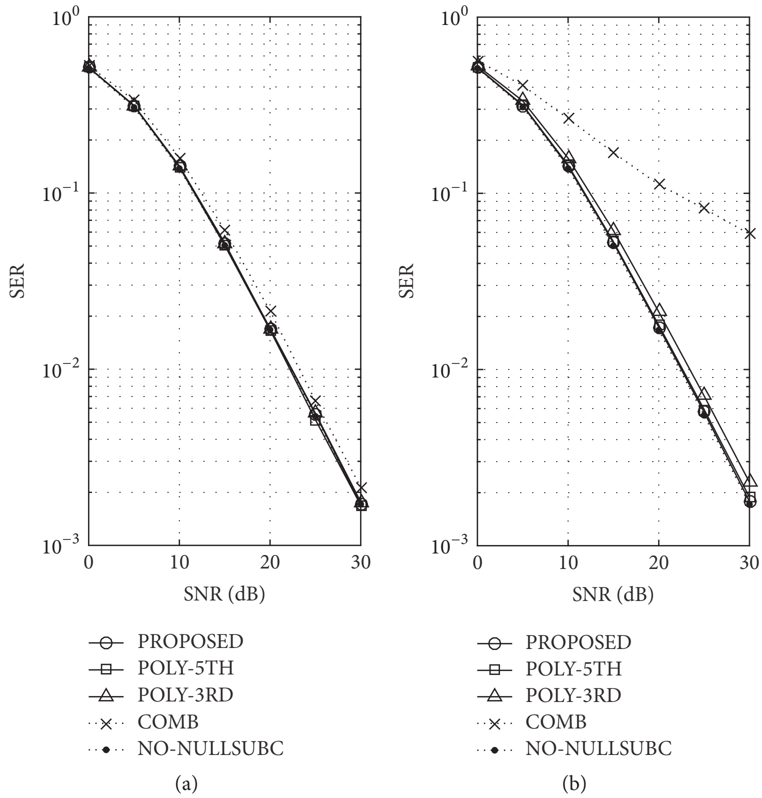

Figure 10: The SERs in terms of SNR in two cases of (a) $N = 512$, $N_a = 470$, and $N_p = 32$ and (b) $N = 1024$, $N_a = 942$, and $N_p = 64$.

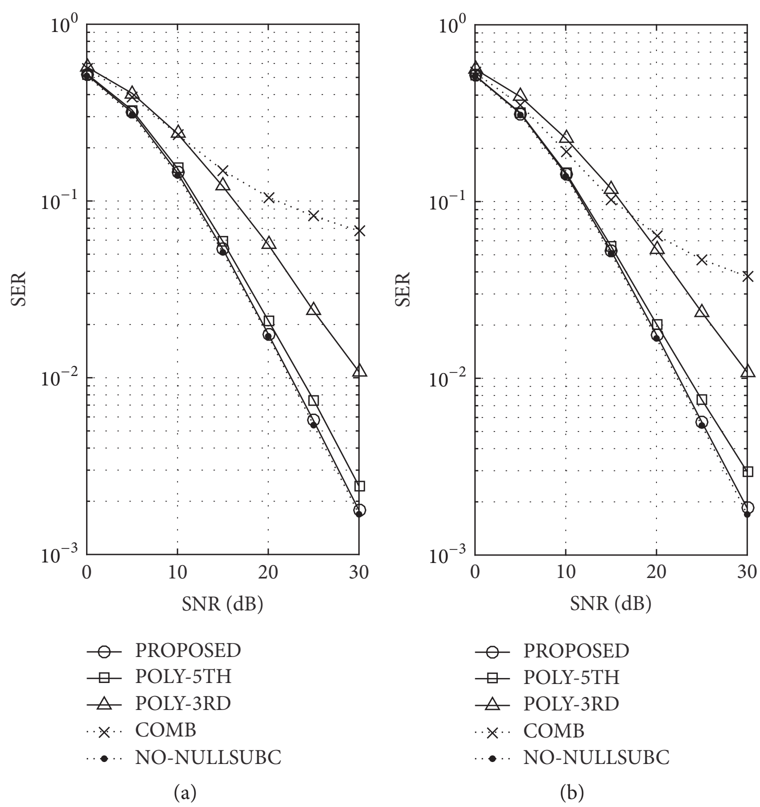

Figure 11: The SERs in terms of SNR in two cases of (a) $N = 2048$, $N_a = 1884$, and $N_p = 128$ and (b) $N = 4096$, $N_a = 3768$, and $N_p = 256$.

where $\mathbf{I}_{N_\mathrm{p}}$ denotes an $N_\mathrm{p} \times N_\mathrm{p}$ dimensional identity matrix. All the eigenvalues of $(1/\widetilde{N}_\mathrm{p})\widetilde{\mathbf{D}}_\mathrm{p}^H\widetilde{\mathbf{D}}_\mathrm{p}$ are equal to one another. It implies that $(1/\widetilde{N}_\mathrm{p})\widetilde{\mathbf{D}}_\mathrm{p}^H\widetilde{\mathbf{D}}_\mathrm{p}$ has the largest possible minimum eigenvalue (i.e., 1). Since NO-NULLSUBC makes $(1/N_\mathrm{p})\mathbf{D}_\mathrm{p}^H\mathbf{D}_\mathrm{p}$ have the largest possible minimum eigenvalue and its pilot density is chosen to be equal to that of COMB, NO-NULLSUBC yields a smaller MSE value than COMB and other pilot allocation schemes when the OFDM block includes null subcarriers. Let $\mathbf{F}$ and $\mathbf{F}_\mathrm{L}$ define an $N \times N$ dimensional discrete Fourier transform matrix and an $N \times N_\mathrm{p}$ dimensional matrix consisting of the first N_p consecutive columns of $\mathbf{F}$, respectively. $\mathbf{F}_\mathrm{L}$ can be written in terms of $\widetilde{\mathbf{D}}_\mathrm{p}$ and $\widetilde{\mathbf{D}}_\mathrm{d}$ as

$$\sqrt{N} \times \mathbf{F}_\mathrm{L} = \mathbf{P} \times \begin{bmatrix} \widetilde{\mathbf{D}}_\mathrm{p} \\ \widetilde{\mathbf{D}}_\mathrm{d} \end{bmatrix}, \tag{A.6}$$

where $\mathbf{P}$ denotes a relevant permutation matrix. Since $\mathbf{F}_\mathrm{L}^H\mathbf{F}_\mathrm{L} = \mathbf{I}_{N_\mathrm{p}}$ and $\mathbf{P}^H\mathbf{P} = \mathbf{I}_{N_\mathrm{p}}$, it follows that

$$\widetilde{\mathbf{D}}_\mathrm{p}^H\widetilde{\mathbf{D}}_\mathrm{p} + \widetilde{\mathbf{D}}_\mathrm{d}^H\widetilde{\mathbf{D}}_\mathrm{d} = N\mathbf{I}_{N_\mathrm{p}}. \tag{A.7}$$

From (A.5) and (A.7), it follows that

$$\frac{1}{\widetilde{N}_\mathrm{d}}\widetilde{\mathbf{D}}_\mathrm{d}^H\widetilde{\mathbf{D}}_\mathrm{d} = \mathbf{I}_{N_\mathrm{p}}. \tag{A.8}$$

Analogously to (9), the MSE vector for the data subcarriers is given by

$$\widetilde{\mathbf{e}} = \sigma^2 \operatorname{diag}\left\{\widetilde{\mathbf{D}}_\mathrm{d}\left(\widetilde{\mathbf{D}}_\mathrm{p}^H\widetilde{\mathbf{D}}_\mathrm{p}\right)^{-1}\widetilde{\mathbf{D}}_\mathrm{d}^H\right\}. \tag{A.9}$$

By substituting the results of (A.5) and (A.8) into (A.9), it can be finally obtained that

$$\widetilde{\mathbf{e}} = \frac{\sigma^2 N_\mathrm{p}}{\widetilde{N}_\mathrm{p}} \operatorname{diag}\left\{\mathbf{I}_{\widetilde{N}_\mathrm{d}}\right\}, \tag{A.10}$$

which shows that all the data subcarriers have the same MSE as $\sigma^2 N_\mathrm{p}/\widetilde{N}_\mathrm{p}$.

Conflicts of Interest

The authors declare that there are no conflicts of interest regarding the publication of this paper.

Acknowledgments

This paper was supported by Konkuk University in 2017.

References

[1] N. Bhushan, T. Ji, O. Koymen et al., "Industry Perspective: 5G Air Interface System Design Principles," *IEEE Wireless Communications Magazine*, vol. 24, no. 5, pp. 6–8, 2017.

[2] S. Adireddy, L. Tong, and H. Viswanathan, "Optimal placement of training for frequency-selective block-fading channels," *Institute of Electrical and Electronics Engineers Transactions on Information Theory*, vol. 48, no. 8, pp. 2338–2353, 2002.

[3] I. Barhumi, G. Leus, and M. Moonen, "Optimal training design for MIMO OFDM systems in mobile wireless channels," *IEEE Transactions on Signal Processing*, vol. 51, no. 6, pp. 1615–1624, 2003.

[4] S. Ohno, "Preamble and pilot symbol design for channel estimation in OFDM," in *Proceedings of the IEEE International Conference on Acoustics, Speech and Signal Processing, ICASSP '07*, pp. III281–III284, USA, April 2007.

[5] R. A. Chougule and P. P. Belagali, "Efficient Use of Null Subcarriers to Reduce PAPR in OFDM System," *International Journal of Innovative Research in Advanced Engineering (IJIRAE)*, vol. 1, no. 9, 2014.

[6] M. Morelli and U. Mengali, "A comparison of pilot-aided channel estimation methods for OFDM systems," *IEEE Transactions on Signal Processing*, vol. 49, no. 12, pp. 3065–3073, 2001.

[7] R. J. Baxley, J. E. Kleider, and G. T. Zhou, "Pilot design for IEEE 802.16 OFDM and OFDMA," in *Proceedings of the 2007 IEEE International Conference on Acoustics, Speech and Signal Processing, ICASSP '07*, pp. II321–II324, USA, April 2007.

[8] Document 5D/TEMP/300 (Rev.1), "Minimum Requirements Related to Technical Performance for IMT-2020 Radio Interfaces," Tech. Rep., ITU Radiocommunications Study Groups, 2017, https://www.itu.int/md/R15-SG05-C-0040/en.

[9] S. Song and A. C. Singer, "Pilot-aided OFDM channel estimation in the presence of the guard band," *IEEE Transactions on Communications*, vol. 55, no. 8, pp. 1459–1465, 2007.

[10] R. J. Baxley, J. E. Kleider, and G. T. Zhou, "Pilot design for OFDM with null edge subcarriers," *IEEE Transactions on Wireless Communications*, vol. 8, no. 1, pp. 396–405, 2009.

[11] S. Ohno, E. Manasseh, and M. Nakamoto, "Pilot Symbol Design for Channel Estimation in OFDM with Null Subcarriers," in *Proceedings of APSIPA Annual Summit and Conference '09*, Sapporo, Japan, 2009.

[12] B. R. Hamilton, X. Ma, J. E. Kleider, and R. J. Baxley, "OFDM pilot design for channel estimation with null edge subcarriers," *IEEE Transactions on Wireless Communications*, vol. 10, no. 10, pp. 3145–3150, 2011.

[13] E. Manasseh, S. Ohno, and M. Nakamoto, "Combined channel estimation and PAPR reduction technique for MIMO–OFDM systems with null subcarriers," *EURASIP Journal on Wireless Communications and Networking*, vol. 2012, no. 1, article A001, pp. 75–85, 2012.

[14] T. Kailath, A. H. Sayed, and B. Hassibi, *Linear Estimation*, Prentice Hall, 2000.

[15] J. C. A. Barata and M. S. Hussein, "The Moore-Penrose pseudoinverse: a tutorial review of the theory," *Brazilian Journal of Physics*, vol. 42, no. 1-2, pp. 146–165, 2012.


Journal of Engineering
The Scientific World Journal
International Journal of Rotating Machinery
Journal of Sensors
Advances in Multimedia
Advances in Civil Engineering
Hindawi
Submit your manuscripts at
www.hindawi.com
Journal of Control Science and Engineering
Journal of Robotics
Journal of Electrical and Computer Engineering
Advances in OptoElectronics
VLSI Design
International Journal of Navigation and Observation
Modelling & Simulation in Engineering
International Journal of Aerospace Engineering
International Journal of Chemical Engineering
International Journal of Antennas and Propagation
Active and Passive Electronic Components
Shock and Vibration
Advances in Acoustics and Vibration